Modeling brain dynamics and gaze behavior: Starting point bias and drift rate relate to frontal midline theta oscillations

Peter J. Castagna [a],[1], Stefon van Noordt [b],[1], Per B. Sederberg [c], Michael J. Crowley [a],*

[a] *Yale Child Study Center, Yale School of Medicine, New Haven, CT 06511, United States*
[b] *Department of Psychology, Mount Saint Vincent University, Halifax B3M 2J6, Canada*
[c] *Department of Psychology, University of Virginia, Charlottesville, VA 22904, United States*

A B S T R A C T

Frontal midline theta oscillatory dynamics have been implicated as an important neural signature of inhibitory control. However, most proactive cognitive control studies rely on behavioral tasks where individual differences are inferred through button presses. We applied computational modeling to further refine our understanding of theta dynamics in a cued anti-saccade task with gaze-contingent eye tracking. Using a drift diffusion model, increased frontal midline theta power during high-conflict, relative to low-conflict, trials predicted a more conservative style of responding through the starting point (bias). During both high- and low-conflict trials, increases in frontal midline theta also predicted improvements in response efficiency (drift rate). Regression analyses provided support for the importance of the starting point bias, which was associated with frontal midline theta over the course of the task above-and-beyond both drift rate and mean reaction time. Our findings provide a more thorough understanding of proactive gaze control by linking trial-by-trial increases of frontal midline theta to a shift in starting point bias facilitating a more neutral style of responding.

1. Introduction

A growing body of work implicates perturbations of frontal and central midline theta oscillations [∼4–8 Hz] as a robust, domain-general neural marker of cognitive control processes (Cavanagh and Shackman, 2015, Cavanagh and Frank, 2014, Eisma et al., 2021). It is believed that there are two independent, but concurrently active, generators of frontal midline theta (FMT) in the anterior cingulate cortex, where the FMT response is thought to not only relate to conflict but also conflict-independent processes associated with response slowing (Töllner et al., 2017, Zuure et al., 2020). Despite the breadth and extent of this work, most cognitive control-related studies rely on behavioral tasks where differences in attentional resources are inferred from button presses. Gaze-contingent eye tracking allows for attention-related cognitive control to be linked more directly to changes in the experimental paradigm. Given the broad interest in visual attention training to target a range of psychiatric disorders (Hallion and Ruscio, 2011, Shagan et al., 2018, Joekar et al., 2017, Javadipour et al., 2018, Archambault et al., 2021, Bell et al., 2009, Finn and McDonald, 2011, Kłosowska et al., 2015, Beard et al., 2012, Mogg et al., 2017, Fodor et al., 2020, Boettcher et al., 2013, Armstrong and Olatunji, 2012, Habedank et al., 2017), it is important to understand how visual attention is controlled to properly design

such trainings. While there is ample evidence how FMT is critical to re-active and proactive control, it is unknown whether these past findings, based on manual responses, generalize to gaze control. Reactive control is characterized by a response to a cue/event in the environment following the initiation of the response process. Proactive cognitive control, in contrast, involves a preparatory process which affects whether the response process is initiated (Aron, 2011). Therefore, studying gaze behavior directly may further our understanding of the cognitive processes central to visual attention training interventions. We propose a first step in this direction by combining trial-by-trial EEG neural dynamics and computational modeling using a cued anti-saccade task to allow for a more nuanced examination of proactive cognitive control, directly studied at the level of gaze behavior.

Theta oscillations increase in power following response errors (Holroyd and Coles, 2002, Gehring et al., 2018, Yeung et al., 2004) and negative feedback (Walsh and Anderson, 2012), in response to unexpected events (Cavanagh et al., 2012, Mas-Herrero and Marco-Pallarés, 2014), during inhibitory control (Nigbur et al., 2012, Nigbur et al., 2011), when resolving competition between different responses (Oehrn et al., 2014), adjusting response strategies to task demands (López et al., 2019, McKewen et al., 2020), and following events that are novel or ambiguous in terms of performance feedback

---

(Sandre and Weinberg, 2019, Wessel et al., 2012). Several studies report that modulation of frontal midline theta (FMT) varies in relation to single trial behaviors, including accuracy (Cohen and Donner, 2013), response adjustments following errors (Kalfaoğlu et al., 2018), reaction times (McKewen et al., 2020), and learning from feedback to adapt future responses (Cavanagh et al., 2010). Stimulation studies offer more direct evidence, as the manipulation of increasing FMT activity has positive impacts on behavior (Klink et al., 2020, Voelker et al., 2021). For example, transcranial alternating current stimulation in the theta range applied over frontal regions results in immediate improvements in behavioral adjustments following errors (Reinhart et al., 2015), not simply attributable to a tradeoff between speed and accuracy (Fusco et al., 2018). Conversely, disrupting frontal theta oscillatory dynamics leads to performance decrements (Reinhart, 2017). Direct evidence that frontal theta dynamics are critical for goal-directed behaviors comes from intracranial recordings. Similar to the scalp derived FMT signatures observed in humans, intracranial recordings taken from single frontal midline neurons in non-human animals reveal the presence of theta oscillations that mediate encoding of stimulus-response mappings (Womelsdorf et al., 2010), error commission (Narayanan et al., 2013), and on-going response adjustments (Womelsdorf et al., 2010, Womelsdorf et al., 2010). Deactivation of medial frontal function results in a reduction in theta to errors and impaired response adjustments following errors (Narayanan et al., 2013). Collectively, these studies suggest that FMT oscillations are indicative of cognitive control processes, perhaps providing a rhythmic temporal structure in the theta range to coordinate activity across neural systems that mediate complex goal-directed behavior (Fiebelkorn and Kastner, 2019).

A critical aspect of adaptive goal-directed behavior is appropriate response preparation. Often cognitive control is partitioned into what is referred to as reactive and proactive control mechanisms (Braver, 2012, Jaffard et al., 2007, Jaffard et al., 2008, Meyer and Bucci, 2016). The former generally refers to a reaction to a cue/event in the environment following the initiation of the response process. Proactive cognitive control, in contrast, involves a preparatory process which affects whether the response process is initiated (Aron, 2011). In non-human animals, FMT oscillations show behavioral selectivity and sensitivity to choice-relevant information—rhythmic theta activity increases prior to a behavioral response and is predictive of stimulus-response mapping choices (Womelsdorf et al., 2010). Similarly, studies on proactive cognitive control in humans also suggest that FMT activity is engaged during response preparation. For example, using a cued (low-/high-conflict) mental calculation task, De Loof and colleagues (De Loof et al., 2019) observed increases in frontal theta power leading up to task onset on difficult trials, which correlated with behavior across participants, and single trials. Other studies report increased frontal theta during the cue-target interval when individuals were made aware (i.e., cue) that the upcoming target trial (i.e., target) required a switch between task sets (Cooper et al., 2015, Cooper et al., 2017, Sauseng et al., 2019). Although evidence is accumulating that FMT supports these context-dependent adjustments in cognitive control, most studies employ cognitive control paradigms requiring a motor response via a button press, one step removed from the gaze behavior under study. In fact, recent work has highlighted the advantage of gaze-contingent eye tracking paradigms when studying cognitive control during multiple-target search (van Driel et al., 2019). Examining the theta dynamics of proactive cognitive control, we previously reported similar findings using a cued anti-saccade task (van Noordt et al., 2017). Participants were informed as to whether the upcoming response probe required a pro-saccade (low-conflict) or an anti-saccade (high-conflict) gaze response (van Noordt et al., 2017). In addition to the well documented increase in post-error theta power, we observed robust FMT activity during the delay period that was greater for correct anti-saccade, relative to pro-saccade, trials (van Noordt et al., 2017). These findings indicate that FMT is engaged during proactive cognitive control, particularly when successfully preparing a challenging behavioral response.

The conventional approach to analyzing task performance involves behavioral summary statistics such as mean reaction time and accuracy, assessed via button-presses. However, these metrics are not well-suited to fully unpack the complex interaction within and among the various brain networks involved in inhibitory control (Cavanagh et al., 2011). Computational approaches (Adams et al., 2016, Collins and Shenhav, 2021) aim to address this problem through modeling task-based behavioral and neural data (joint modeling) into separable processes. The goal of this approach is to identify whether these processes deepen our understanding of the mechanistic explanations for perturbed cognitive functioning. Process models, such as the drift diffusion model, provide additional information beyond traditional measures (mean reaction time) about underlying latent cognitive processes and their intraindividual variability across experimental trials (Cavanagh et al., 2011, Ratcliff, 1978, Ratcliff, 1985, Ratcliff and Childers, 2015, Ratcliff and McKoon, 2008, Ratcliff and Rouder, 1998, Ratcliff et al., 2016, Stone, 1960). More recent advances in computational approaches have led to the development of programs to model behavior from a hierarchical drift-diffusion framework (Wiecki et al., 2013). These model-based approaches have proven useful in delineating underlying latent cognitive processes of complex task performance, trial by trial (Cavanagh et al., 2011). A handful of studies have demonstrated greater precision and specificity when relating task performance to behavior by applying a drift-diffusion approach to inhibitory control as measured by the anti-saccade task (Cavanagh et al., 2011, Tannous et al., 2019, Wiecki et al., 2016). The models include drift rate, decision threshold, and starting point bias latent parameters to characterize cognitive processes as latent variables thought to underlie inhibitory control. For example, in a study of individuals with comorbid cocaine/alcohol use disorders, Tannous et al. (2019) found that, compared to controls, individuals with substance use disorder demonstrated a decrease in subjective difficulty (i.e., larger drift rates, more efficient processing) during cocaine-cued trials of the modified anti-saccade task when modeled from a drift diffusion framework. In another study, traditional metrics (e.g., reaction time, error rates) could not differentiate control participants from those with pre-Huntington's disease, while latent computational modeling parameters (i.e., drift rate, decision threshold) provided increased specificity in correct classification (Wiecki et al., 2016).

To our knowledge, only one study to-date has leveraged computational modeling to relate changes in theta dynamics to *trial-by-trial changes* in cognitive control (Cavanagh et al., 2011). The results of this study showed that trial-to-trial FMT activity predicted an increased threshold for evidence accumulation (i.e., decision threshold) during conflict. Moreover, after deep brain stimulation of the subthalamic nucleus in patients with Parkinson's disease, this relationship was found to be reversed, resulting in impulsive responding; increasing FMT was associated with a reduction of the decision threshold during conflict (Cavanagh et al., 2011). However, studies modeling gaze-contingent proactive cognitive control have primarily focused on drift rate and decision threshold parameters, seldomly examining whether the inclusion of the starting point bias parameter improves model fit. From our viewpoint, it is conceivable that the strength of the prepotent response is captured, at least partially, by a general bias towards a pro-saccade (low conflict) response; while less information is needed for compulsory pro-saccade (expediating the more common task response), more evidence accumulation is needed for an anti-saccade (high conflict). It would follow that a burst FMT, following the preparatory cue, may facilitate overcoming this bias to accurately respond during high-conflict trials.

1.1. Current study

While literature strongly indicate that theta rhythms are indicative of the need for a spontaneous controlled behavioral response (i.e., reactive cognitive control) (Cavanagh and Shackman, 2015), and our recent

work suggests that this neural signature may relate more to context-dependent adaptations in cognitive control (i.e., proactive cognitive control) (van Noordt et al., 2017), the neurophysiological underpinnings of controlled (proactive) gaze behavior are not well understood. The cued anti-saccade task is well suited to examine the links between theta and proactive cognitive control, as saccades are the fastest and perhaps the most prepotent behaviors. Here we apply a cued anti-saccade task to model changes in theta dynamics and trial-by-trial performance assessed via gaze behavior. We posit that distinct parameters of the drift diffusion model (that reflect different, discrete aspects of inhibition) will relate to the trial-by-trial changes in theta oscillatory dynamics. Consistent with similar past work (Tannous et al., 2019, Wiecki et al., 2016, Cavanagh et al., 2014), we hypothesize that individual differences in FMT will relate to changes in participant's drift rate (response efficiency), decision threshold (amount of evidence needed for a decision), and starting point bias (amount of evidence for one decision inversely affecting the alternative) during the course of this proactive cognitive control task. To our knowledge, previous work has not specifically examined the drift diffusion starting point bias parameter as it relates to performance on the anti-saccade; however, recent work has found the inclusion of the bias parameter useful in modeling an orienting response (Jha et al., 2022). Therefore, we examined whether the addition of bias improved model fit in an exploratory nature. Finally, in an effort to demonstrate the utility of deconstructing participants behavior through computational mathematical modeling, we posited that drift diffusion model parameters would predict mean FMT during the anti-saccade task, above-and-beyond that of reaction time alone.

2. Methods

2.1. Participants

Twelve healthy young adults participated in the current study, all of whom were right-handed and had normal or corrected-to-normal vision. One participant was excluded due to excessive movement and muscle artifacts, resulting in more than 60% of in-task time being flagged during automated pre-processing. The final sample of 11 participants included seven 7 males and 4 females, with a mean age of 25 years (SD = 2.87 years). Participation was voluntary and involved no monetary incentives. The study received clearance from the Brock University Bioscience Research Ethics Board and all participants provided informed consent.

2.2. Cued pro-/anti-saccade delay task

Participants completed a cued anti-saccade task where they were required to make pro-saccades and anti-saccades to peripheral probes. For the duration of the task, three squares remained on the screen: a central square where the trial type cue was presented, and two peripheral squares (left and right) where the saccade response probes appeared (see Fig. 1). Trials were initiated after participants focused their gaze behavior on the central square for 200 ms, at which point a fixation cross was presented for 50 ms. The color of the fixation cross was either white or black and signaled whether that trial required a pro-saccade (e.g., white fixation) toward, or an anti-saccade (e.g., black fixation) away from the peripheral response probe. After a fixed delay of 800 ms the response probe flashed for 50 ms in one of the peripheral squares. A fixation of at least two consecutive cycles (~33 ms) on a peripheral square was required for saccade responses to be logged. Immediately following the saccade response, feedback was presented for 200 ms in the form of a check mark for correct responses or an "X" for incorrect responses.

Features of this cued anti-saccade task were modeled from a response cueing paradigm (Roger et al., 2010, Mensen and Khatami, 2013), which includes multiple response contexts that varied in the predictability of anti-saccade trials. For the current study we focus on the response context that included a combination of both pro- and anti-saccade trials. The color of the fixation cross indicating pro-saccade and anti-saccade

trials was counterbalanced across all participants and peripheral probes appeared equally at left and right locations. A total of 192 pro-saccade and 128 anti-saccade trials were used in the current study. The imbalance is due to the blocked structure of the task, similar to a go/no-go task. See Fig. 1 for a summary of trial details.

During data collection participants were seated 16 inches (40.64 cm) from the presentation monitor with their chin secured in a chin rest that was placed at a fixed height to minimize neck tension, head movements, and changes in visual angle to the screen during the task. The approximate visual angle was 0.57 degrees for the saccade cue, 1.72 degrees for borders, 0.57 degrees for error feedback, and 0.59 degree for correct feedback. The distance, in visual angle, between the response cue and peripheral probes was 14.6 degrees. This study relied on the integration of the E-Prime (version 2.0, Psychology Software Tools, Inc.), Smart Eye Pro (60 Hz sampling rate: version 5.8, Smart Eye AB), and Net Station (version 4.5.1, EGI, Inc.) for stimulus presentation, eye-tracking, and EEG acquisition.

2.3. Electrophysiological recordings and data reduction

EEG data were acquired using a 128-channel HydroCel Geodesic Sensor Net (HCGSN; EGI, Inc.), equipped with Ag/AgCl electrodes, and a 300 series amplifier. Signa Gel (Cortech Solutions, Inc.) was used as an electrolyte medium. Impedances were verified at 100 kOhms or lower prior to recording. Data were acquired at a sampling rate of 500 Hz, with a 100 Hz low pass filter, 0.1 Hz high-pass and referenced online to site Cz.

A series of automated pre-processing procedures were executed in Octave 3.6.3 on the Shared Hierarchical Academic Research Computing Network (SHARCNet). The preprocessing trajectory involved flagging channels and time points that reflect spatial and temporal nonstationarity. The pre-processing stream follows closely the steps described previously (Desjardins and Segalowitz, 2013, Desjardins et al., 2021, van Noordt et al., 2015). In-task time was distinguished from out-task time (e.g., instruction period, task lead up, breaks) and the following procedures were performed only on in-task time points. The continuous EEG was filtered from 2 Hz to 30 Hz and re-referenced to the average. This filtering was done as nonstationary artifacts tend to be made up of large, low frequency oscillations (e.g., movement artifact and sweat artifacts), and ICA decompositions are more reliable when a high pass filter is applied to the data [e.g., 1–2 Hz; (Debener et al., 2010, Winkler et al., 2015)]. The data were put through a series of common criteria functions to flag signals or time points based on a specific property (e.g., voltage variance). This process involved calculating the measure of interest, comparing the measure against a distribution, and assessing whether the channel or time point should be flagged as an outlier. First, the continuous data were windowed into 50% overlapping 600 ms windows. For each of these windows the maximum correlation coefficient r of each channel and its three nearest neighbors was calculated to yield n channel correlations. The 99% confidence interval of the r values for each window was calculated and a given channel was flagged if the r was outside the 99% confidence intervals and was flagged for the duration of the recording if it was deemed an outlier in more than 10% of time windows. Bridged electrodes were identified using a composite measure to identify high and relatively invariable correlations between neighboring channels, specifically dividing each channel's mean r value by its standard deviation. Channels were flagged if their composite score was greater than 8 standard deviations from the 25% trimmed mean of the composite scores across channels. The maximum neighbor correlation was then recalculated, and the 99% confidence interval was taken for each channel across the time windows. The time window was flagged if the r value was lower than the 99% confidence interval for a given channel. The time window was flagged for removal if more than 10% of the channels were considered outliers.

The data were concatenated back into a continuous signal with discontinuities marked by boundary events. An initial Infomax ICA de-
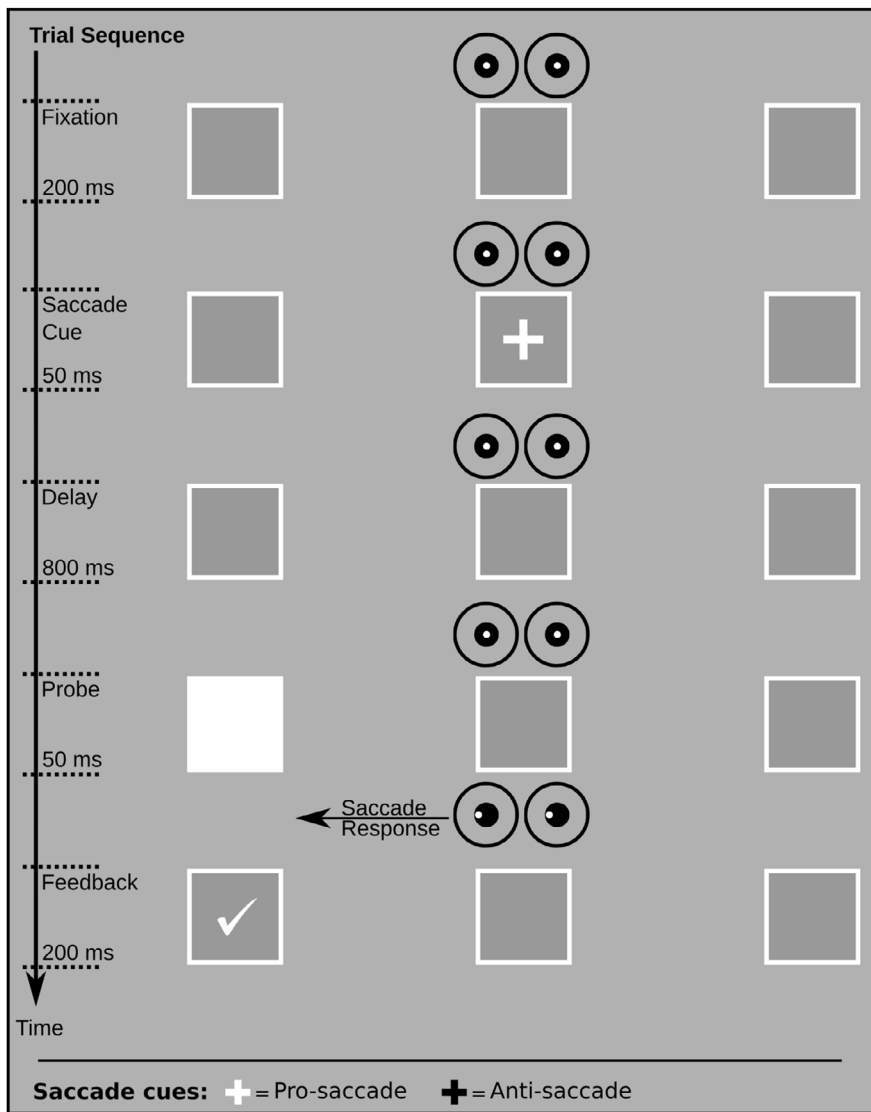
Fig. 1. Saccade trial sequence. Central fixation was required (200 ms duration) in order to initiate the trial. The saccade cue was presented centrally (50 ms) and indicated whether the current trial required a pro-saccade (i.e., look toward) or an anti-saccade (i.e., look away) response. A fixed delay of 800 ms followed before the presentation of the peripheral probe (50 ms) on either the left or right of the screen. Feedback was presented (200 ms) once the participant fixated on one of the peripheral probe locations for a minimum of ∼33 ms (2 consecutive cycles, 60 Hz sampling rate).

composition was performed, and the component time-course activations were used to identify additional time periods for rejection. Specifically, the continuous data were again windowed into 50% overlapping 600 ms windows and the standard deviation of activation was calculated for each IC in each time window. The 99% confidence interval of the standard deviation was calculated for each IC across time windows and the same flagging and rejection criteria used for channel activation was applied. The data were concatenated back into the continuous signal and a second ICA was then applied to the remaining continuous signal that was not flagged in order to produce a more stable decomposition as the training data does not include time periods with unusually high levels of activation in at least 10% of the components. A single dipole was fit to each IC (dipfit plug-in for EEGLab) (Oostenveld et al., 2011). ICs were removed if the residual dipole variance was greater than 15% or manual review of their topographies and continuous activation revealed sources of known biological (i.e., EMG, ECG, EOG) or single channel artifacts (e.g., line noise). We have found a semi-automated approach enhances data retention and signal quality compared to a fully automated flagging procedure (Desjardins et al., 2021). The flagged time points and non-cortical ICs were then purged to remove them from the data, the ICA weights were re-applied to the original time series. The remaining signal was filtered 1 to 30 Hz and re-referenced to the average of 19 interpolated sites. Across subjects an average of 12 cortical ICs ($SD = 4.42$,

ranging from 6 to 21) were retained. Overall, the EEG recordings in the remaining 11 participants were stable based on the automated procedures, such that an average of 94.51% ($SD = 5.31$%) of the in-task time was retained with all participants having more than 80% of in-task time retained (min = 83.65%, max = 97.86%).

2.4. Functional classification of independent components

From the remaining cortical ICs, we classified in each participant those ICs having spatial field projections and functional dynamics representing known medial EEG frontal sources by isolating ICs with a fronto-central medial topography that accounted for the spatial variance in the global field amplitude for the difference between error and correct trials, as these evoked responses are known to reflect medial frontal activity during performance monitoring (van Noordt and Segalowitz, 2012). In each participant, we ranked remaining cortical ICs based on their percentage of variance accounted for in the difference between error and correct responses associated with the error-related negativity and feedback related negativity. Percentage of variance accounted for reflects the total spatial variance (i.e., all cortical ICs projected back to the scalp) minus the variance of the current IC (projected back to the scalp), divided by the total scalp variance. In this process, ICs were sequentially added based on their contribution in accounting for the spatial vari-

ance in the global field amplitude until they accounted for at least 60% of the spatial variance at the scalp. For two participants, this criterion was increased to include the medial frontal projecting IC that differentiated between correct and error trials (70% [$n = 1$], 80% [$n = 1$]). In seven participants, a single medial frontal project IC was found to contribute to the spatial scalp variance that differentiated correct from error trials. The remaining four participants had 2 medial frontal projecting ICs and the mean projections of these two ICs was used. A similar approach has been used to classify medial frontal ICs that differentiate between error and correct responses (Wessel et al., 2012, Gentsch et al., 2009, Hoffmann and Falkenstein, 2010, Roger et al., 2010) or stimulus cues that signal potential changes in response demands (van Noordt et al., 2015). The classification of ICs was based on functional dynamics to task events that were temporally distinct from the activity that occurred during the delay period (i.e., between saccade cue and peripheral probe) that was used for hypothesis testing. For the purpose of discriminant validity and specificity of the medial frontal ICs representing task-based changes in response preparation, we also performed analyses on the residual EEG data which reflects all remaining cortical ICs that were not classified as representing a medial frontal source.

2.5. Time-frequency decomposition of classified independent components

Epochs were time-locked to the onset of saccade cues from -2000ms to 2850ms, separately for pro- and anti-saccade trials. Following preprocessing, there was an average of 158 and 96 trials available for pro and anti-saccade conditions, respectively. The correlation of trial numbers between the conditions was strong ($r(10) = .88$, $p < .001$), indicating that overall levels of artifact identified during pre-processing were similar across participants. The single trial event-related dynamics for each IC in the medial frontal cluster were convolved using complex Morlet wavelets (EEGLab function *newtimef*) to generate spectral power estimates from 1–30 Hz. For purposes of convergent validity, we also extracted theta for the residual EEG data. Specifically, theta power was calculated for all ICs excluding the classified medial frontal ICs. Examining the spectral power dynamics in the residual EEG can help to further establish whether the activity in classified sources is important for single trial modulation of behavior based on the extent to which it uniquely relates to task relevant behaviors. In addition, we implemented a robust approach to assess the spatial-temporal dynamics of theta power for both the fronto-central and residual ICs. Specifically, we performed independent samples, two-tailed cluster permutation tests using threshold free cluster enhancement (Mensen and Khatami, 2013). Threshold free cluster enhancement is similar to other established cluster-based approaches (e.g., cluster max, cluster mass) (Bullmore et al., 1999, Groppe et al., 2011, Groppe et al., 2011, Maris, 2004, Maris and Oostenveld, 2007), with the exception that threshold free cluster enhancement considers the spatial and temporal dependencies in the EEG data by being sensitive to both strong(er)-narrow and weak(er)-broad effects, which minimizes the trade-offs between sensitivity and control of Type I error rate or the use of potentially arbitrary cut-offs for defining cluster thresholds. Threshold free cluster enhancement is capable of effectively maintaining family-wise alpha at 0.05 and control Type I error rates for multiple comparisons across all EEG channels and time points. Based on the results from Mensen and Khatami (Mensen and Khatami, 2013), we set E = 0.66 and H = 2. See Fig. 2 for a summary of the IC functional classification and theta dynamics.

2.6. Statistical analyses

2.6.1. Drift diffusion modeling

We chose to conduct the specific sequential sampling method known as drift diffusion modeling (Ratcliff, 1985, Ratcliff and Childers, 2015, Ratcliff and McKoon, 2008, Ratcliff and Rouder, 1998, Stone, 1960, Smith and Ratcliff, 2004), as it has been established as the standard for modeling response-time data from simple two-alternative forced

choice decision-making tasks (Smith and Ratcliff, 2004) (see Fig. 3). Specifically, hierarchical Bayesian parameter estimation using Markov-chain Monte-Carlo was used to estimate posterior distributions of the drift-diffusion parameters via the Hierarchical Drift Diffusion Modeling (HDDM 0.8.0) Python toolbox (Wiecki et al., 2013). Due to our interest in the inclusion of the starting point bias parameter as potentially capturing individuals' prepotent (pro-saccade) response, stimulus-coding was utilized for all models. It is important to note that this deviates from the conventional interpretation of the bias parameter. Here, the starting point bias is conceptualized as facilitating in a stimulus-response mapping; thus, from this viewpoint, individuals need to overcome the bias to provide the prepotent pro-saccade response created by the true bias in the stimulus mapping (e.g., more pro-saccade versus anti-saccade trials).

To gain a deeper understanding of how anti-saccades can be reflected in cognitive control performance, we were interested in three drift diffusion model parameters across the two task conditions: drift rate, response threshold (Cavanagh et al., 2011, Tannous et al., 2019, Wiecki et al., 2016, Nayak et al., 2019), as well as starting point bias (Jha et al., 2022) using stimulus-coding. First, two null models (both assuming that parameters do not vary as a function of pro- versus anti-saccade conditions) only differed on whether they included the bias parameter to determine if the inclusion of this optional parameter improved overall model fit. Next, depending on the best-fitting null-model (i.e., with or without the bias parameter), a series of models were compared varying on either the two (i.e., drift rate and decision threshold) or three (i.e., drift rate, decision threshold, and starting point bias) parameters split by task condition to determine the best-fitting model.

Group models do not have the power to detect the effect of condition on a within-subject effect (e.g., condition on an individuals' parameter estimate), as there would be large posterior variance in all of the drift rates, for example, that overlap with one another. The within-subject model, in contrast, estimates a large variance in the intercept while allowing the model to infer a non-zero effect of condition with high level of precision. Within-subject models were then conducted to further probe the effect of task condition on individual subjects' parameter estimates; a particular parameter's intercept is used to capture overall performance in the low-conflict condition as a baseline, which is then expressed relative to the high-conflict condition. Within subject models were run separately for each split parameter from the best-fitting group model.

2.7. Within-subject drift diffusion regressor models

On the basis of past work with similar cognitive control tasks (Cavanagh et al., 2011), we examined the within-subject effects of trial-by-trial changes in frontal midline theta (FMT) on diffusion parameters while also allowing for different difficulty levels to exert influence via a hierarchical drift diffusion regression model. Drift diffusion parameters and the effect of participants' trial-by-trial changes in FMT during the anti-saccade task on the parameters of interest were estimated within the same hierarchical Bayesian framework. The regressor model allowed for trial-by-trial influences of FMT on parameters across the entire task to be examined within-subject. The formula: *drift diffusion parameter* $= a + e\theta \times \theta$, where a reflects the intercept, $e\theta$ reflects the effect of FMT on the parameter of interest, and θ reflects the single trial-estimated theta-band activity. To test the assumption that potential effects are specific to FMT, a second drift diffusion regression model was created in an identical manner predicting *residual FMT*. To do so, Bayesian hypothesis testing was employed, where the probability mass of the respective parameter region (e.g., percentage of posterior samples less than zero) was analyzed to provide a direct probability measure (i.e., P), which is interpreted in a similar way to frequentist *p*-values.

For each model (group as well as within-subject), 30,000 samples were generated from the posteriors with the first 10,000 serving as a burn-in, every second sample was discarded as part of a thinning procedure, and four chains were run. Trace, autocorrelation, and
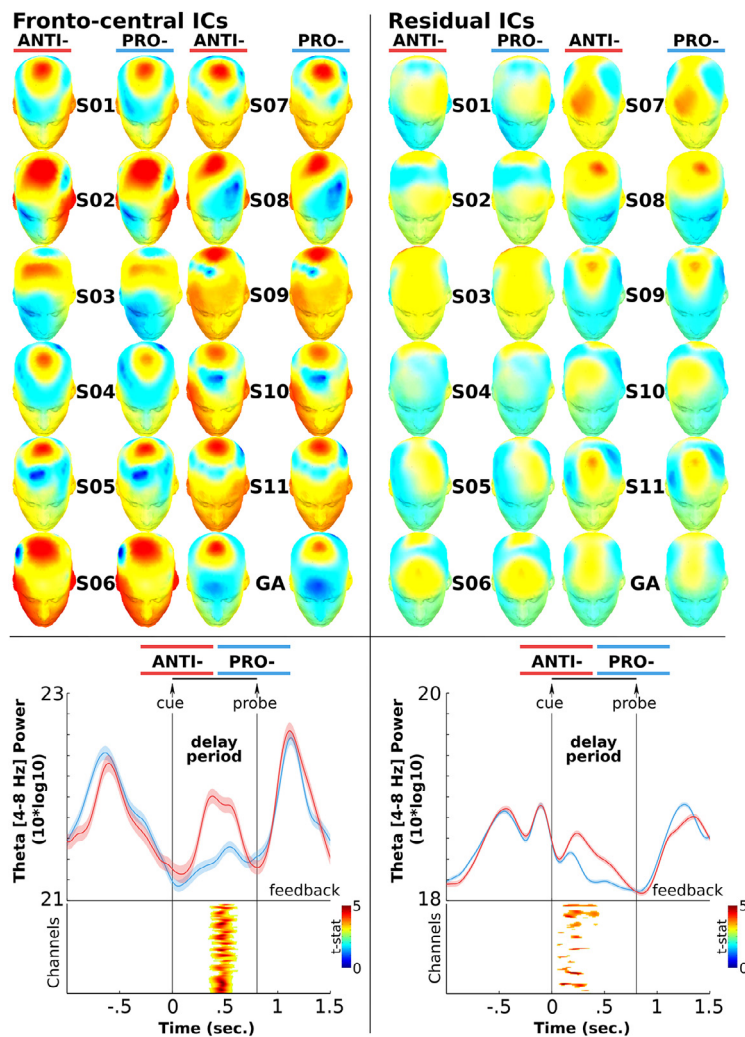
Fig. 2. Top panel shows topographical maps for fronto-central (left) and residual (right) ICs for both anti (orange) and pro-saccade (blue) conditions. The bottom panel shows theta power waveforms for fronto-central (left) and residual (right) ICs, with vertical lines denoting the delay period between the onset of the saccade cue (time 0 ms) and the peripheral response probe (time 800 ms). The heat maps show the channel (y-axis) by time (x-axis) array for robust theta differences between conditions ($p < .05$), as determined by threshold free cluster enhancement and non-parametric permutation testing using Monte Carlo (masked for significance).

marginal posterior plots of model parameters were inspected to informally test model convergence. The Gelman-Rubin statistic (Gelman and Rubin, 1992) was calculated to provide a method to formally test convergence by comparing within- and between-chain variance of different runs of the same model. Convergence was assessed for all models examined. This statistic should be close to 1.0 if the samples of the different chains are indistinguishable. The Gelman-Rubin statistic was calculated (10,000 iterations, 1000 burn-in each) for each participant and found to be < 1.1. The deviance information criterion (Dickerson and Kemeny, 2004) and posterior mean deviance (Dickerson and Kemeny, 2004, Spiegelhalter et al., 2002) were used for model comparison, where lower scores indicate a better fitting model. Deviance information criterion (Dickerson and Kemeny, 2004) values >10 has been used by others as indicating a particular model meaningfully improved fit (Nayak et al., 2019, Herz et al., 2016). The hierarchical drift diffusion model package was run in Python and correlational analyses were computed in R. Data and scripts can be obtained from our online data repository.

2.8. Correlation & regression analyses

We examined the relationship between individual parameter estimates of the best fitting model, neural signatures (i.e., FMT), and task performance (i.e., percent correct, reaction time, RT) via Pearson correlations. Next, a single regression model predicting FMT power was conducted where the first step included participants' reaction time dif-

ference score during the task, and the second step included drift rate and bias difference scores. Difference scores were calculated to provide a metric for the within-subject changes in performance between task conditions and were all calculated in the same manner; mean pro-saccade trial (low conflict) scores minus anti-saccade trial (high conflict) scores. These analyses were included to test the assumption that drift diffusion model parameters would provide additional information regarding proactive control above-and-beyond simple reaction time.

3. Results

3.1. Behavioral

Behaviorally, as reported in (van Noordt et al., 2017) participants did significantly better during pro- ($M = .96$, $SD = .06$) when compared to anti-saccade ($M = .85$, $SD = .15$) trials, $t(10) = 4.07$, $p < .01$, Cohen's D = 1.23. In contrast, there was not a significant difference between reaction times during the pro- ($M = .30$, $SD = .03$) and anti-saccade ($M = .32$, $SD = .10$) conditions, $t(10) = -1.85$, $p = .09$, Cohen's D = -.56.

3.2. Drift diffusion model convergence

We fit participants' performance to the most widely used mathematical model of two-alternative forced-choice decision-making: a drift diffusion model (Ratcliff and Childers, 2015, Ratcliff and McKoon, 2008, Ratcliff and Rouder, 1998, Stone, 1960). To assess model convergence,
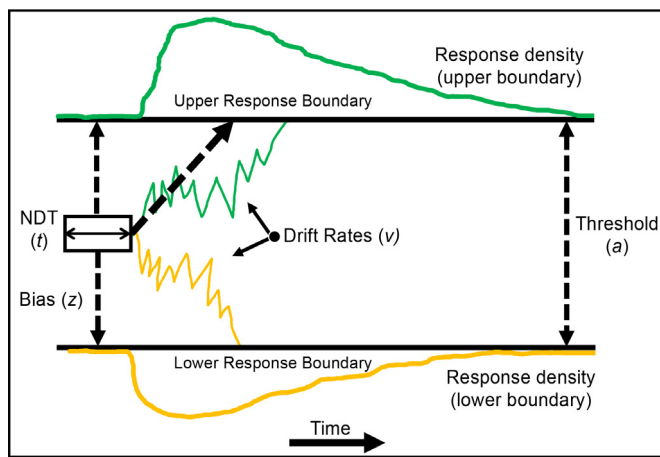
Fig. 3. Simulated trajectories of the two drift-processes (blue and red lines). Evidence is noisily accumulated over time (x-axis) where the (average) drift-rate (v) continues until it reaches one of two boundaries, with a degree of separation defined by threshold (a), is crossed and a response is initiated. An individual's starting point along the y-axis is defined by the bias (z) parameter. Upper (green) and lower (orange) panels refer to density plots over for the two responses. The horizontal solid boxed line in the beginning of the drift-processes indicates the non-decision time (t), NDT, where no accumulation happens. Colored lines within the boundaries indicate two hypothetical trials. While simulation data is depicted here, hierarchical drift diffusion model uses a closed-form likelihood function.

Table 1

Convergence statistics of models examined. *Note.* DIC = deviance information criterion; pD = posterior mean of the deviance minus the deviance of the posterior means; bold = best fit; Δ Null Model = change in DIC/pD from null model with bias; Δ Best Fitting Model = change in DIC/pD from model 8.

Model	DIC	pD
1. Null Model (Without Bias)	-4127	31
2. Null Model (With Bias)	**-4260**	**37**
3. Threshold Only Model	-4426	41
Δ Null Model	-166	+4
Δ Best Fitting Model	+474	-17
4. Drift Only Model	-4455	42
Δ Null Model	-195	+5
Δ Best Fitting Model	+455	-16
5. Bias Only Model	-4711	46
Δ Null Model	-451	+9
Δ Best Fitting Model	+189	-12
6. Bias & Threshold Model	-4765	46
Δ Null Model	-505	+9
Δ Best Fitting Model	+135	-12
7. Drift & Threshold Model	-4640	51
Δ Null Model	-380	+14
Δ Best Fitting Model	+260	-7
8. Drift & Bias Model	**-4900**	**58**
Δ Null Model	**-640**	**+21**
Δ Best Fitting Model	**0**	**0**
9. Drift, Threshold, Bias Model	-4850	59
Δ Null Model	-590	+22
Δ Best Fitting Model	+50	+1

we started with a visual inspection of the trace, autocorrelation, and the marginal posterior for the parameters. There were no major deviations in trace, such as drifts or large jumps, across parameters. Similarly, autocorrelation of all parameters dropped to zero rather quickly, well smaller than 50, when considering the influence of past samples. Finally, the histograms indicate all parameters are fairly normally distributed (See Fig. 4). Consistent with informal evidence of model convergence, all participants included in our analyses had an Gelman-Rubin statistic ≤ 1.1, suggesting that the samples of the four different chains were indistinguishable and again provide support for model convergence.

The standard drift diffusion model includes the drift rate, decision threshold, and non-decision time parameters and includes an option for including a starting point bias parameter (Wiecki et al., 2013). The response bias is captured by a change in starting point of the drift process. Therefore, we first set out to compare two null models to determine whether the inclusion of the bias parameter along with the three standard drift diffusion parameters [(Voss et al., 2004) and non-decision time] improves overall model fit. We use the null model to refer to the simplest model that does not allow parameters to vary by condition. The purpose of this comparison was to determine if the subsequent model variations examined would focus on the three- or four-parameter drift diffusion model. As shown in the first two rows of Table 1, the four-parameter model that included the bias parameter was a better fit to participants' anti-saccade task performance.

Next, a series of models were constructed differing on which a combination of drift rate, decision threshold, and bias parameters were split by low- and high-conflict conditions (i.e., pro- and anti-saccade). Splitting parameters by task condition creates different parameter estimates for each condition for each participant. Seven models (i.e., a decision threshold only, drift rate only, bias only, bias and decision threshold, drift rate and decision threshold, drift rate and bias, and finally a drift rate, decision threshold, bias model) were examined to explore which latent parameters, when allowed to vary by task condition, provide the best fit to participants' performance. Table 1 provides the fit statistics of the seven models examined. Results indicated that the model that allowed both the drift rate and bias parameters to vary by condition provided the best fit to the behavioral data. While model nine had a

slightly greater pD value (i.e., 59 versus 58), we gave preference to model parsimony when model comparison metrics slightly diverged. Specifically, when compared to the null model with bias, the best fitting null model, where no parameters were allowed to vary as a function of condition, the deviance information criterion and the pD were both meaningfully lower (ΔDIC = -640, ΔpD = -637), where lower values indicate better model fit. Fig. 4 (top) provides a visualization of the posterior probability of the drift rate (pro-saccade: $M = 4.46$, $SD = .70$; anti-saccade: $M = 7.76$, $SD = .74$) and bias (pro-saccade: $M = 0.77$, $SD = .04$; anti-saccade: $M = 0.47$, $SD = .07$) parameters split by task condition. Bayesian hypothesis testing indicated that both drift rate ($P = .001$) starting point bias parameter ($P = .009$), meaningfully differed by condition. Thus, the parameters were extracted from this best-fitting model to examine their relationship with FMT power during the anti-saccade task (Fig. 5).

Within-subject models are helpful to further explore the effects of a task condition on individual subjects' parameter estimates; the intercept is used to capture overall performance in the pro-saccade (low-conflict) condition as a baseline and expressed relative to the anti-saccade (high-conflict) condition. A within-subject model was conducted in the same manner as the group model. As shown in Fig. 4 (bottom), the drift rate intercept, referring to the low-conflict condition, is positive, as is the within-subject effects of the high-conflict condition (i.e., anti-saccade), and neither overlap with zero (both $P < .00001$). In contrast, the within-subject effects of the high-conflict condition (i.e., anti-saccade) on the bias is negative, moving the starting point closer to the boundary initiating an anti-saccade response; the intercept (i.e., pro-saccade, low-conflict condition) is entirely positive, and, again, neither overlap with zero (both $P < .00001$). Taken together, we found a strong positive bias in the low-conflict condition, suggesting that participants are performing a pro-saccade with more ease, as less evidence is necessary to cross the pro-saccade threshold. In the high conflict condition, there is a negative bias with respect to the intercept, providing a buffer such that participants are less prone to (incorrectly) perform a pro-saccade. IT is worth mentioning, however, that the overall bias is still relatively neutral (0.4).These results indicate that the cued high-conflict stimuli (i.e., anti-saccade trials) increased processing efficiency (i.e., drift rate) and facilitated a shift in starting point bias.
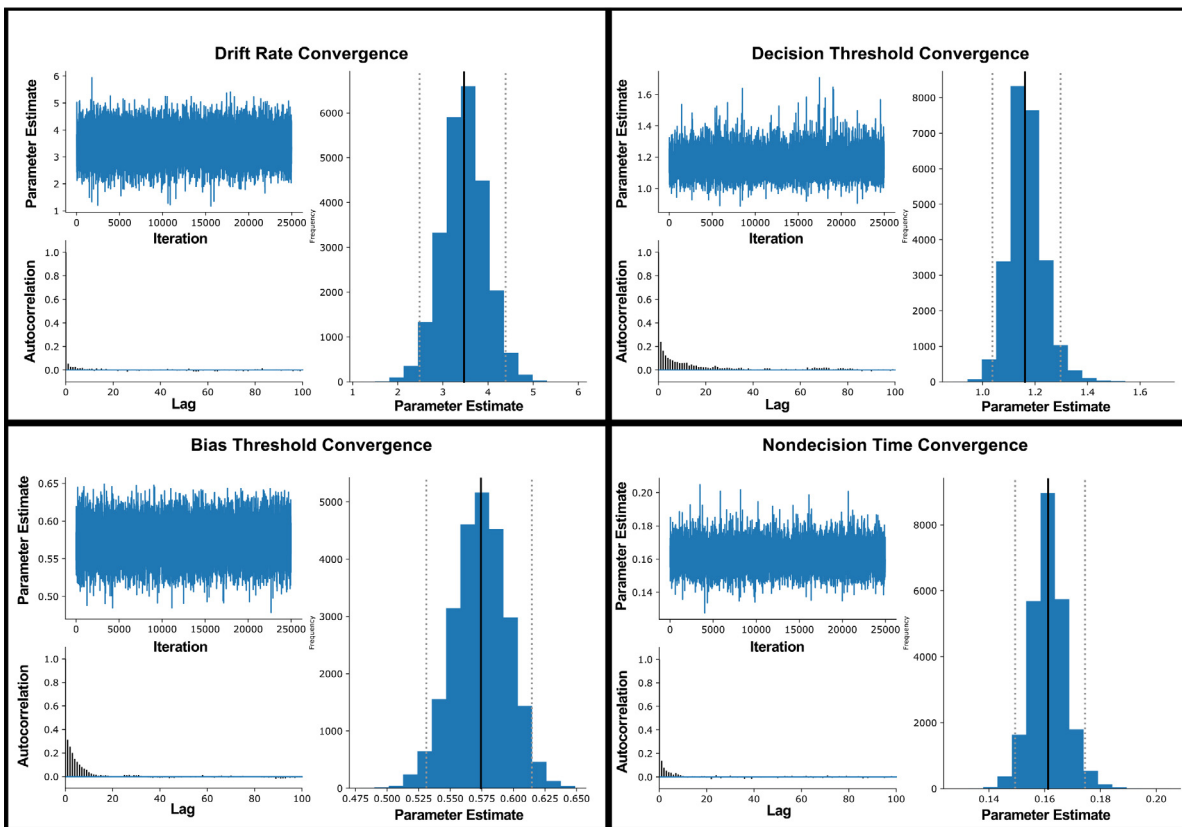
Fig. 4. Posterior plots for the group mean of the threshold (top right), drift rate (top left), bias (bottom left), and non-decision time (bottom right) parameters of the null model, which were nearly identical to those of models allowing parameters to vary by condition. Posterior trace (upper left in lay), autocorrelation (lower left in lay), and marginal posterior histogram (right in lay), where the solid black line denotes posterior mean and dotted black line denotes 2.5 and 97.5% percentiles, are provided.

Table 2
Correlations among drift diffusion parameters, anti-saccade task performance, and frontal midline theta. *Note.* bold = $p < .01$; Anti = anti-saccade trials; Pro = pro-saccade trials; Δ = Difference; FMT = frontal midline theta.

	1.	2.	3.	4.	5.	6.	7.	8.	9.	10.	11.	12.	13.	14.
1. Drift Rate (Pro)	–													
2. Drift Rate (Anti)	.42	–												
3. Bias (Pro)	-.64	.01	–											
4. Bias (Anti)	.36	-.58	-.42	–										
5. Threshold	.23	**.69**	-.17	-.28	–									
6. Non-decision Time	.00	-.22	.30	.40	-.20	–								
7. ΔDrift Rate	.36	**-.69**	-.52	**.89**	-.53	.23	–							
8. ΔBias	-.65	.18	**.89**	-.64	-.06	.14	**-.70**	–						
9. Performance	.59	**.82**	-.15	-.20	**.76**	-.05	-.38	-.07	–					
10. Reaction Time	-.38	-.30	-.10	.17	.39	.23	.01	-.13	-.05	–				
11. ΔReaction Time	-.21	.12	-.34	-.54	.11	-.58	-.29	-.13	-.17	.09	–			
12. FMT (Pro)	**.76**	-.19	**-.75**	-.27	-.09	.25	-.42	**-.71**	-.44	.17	.11	–		
13. FMT (Anti)	.40	**.69**	.29	.49	-.42	.24	.39	.10	-.46	.23	.53	.38	–	
14. ΔFMT	.41	.38	.49	-.66	.25	.05	**.72**	-.61	.05	.02	.33	.66	-.45	–
15. Residual FMT	.37	.09	-.27	.07	.10	.22	.20	-.25	.33	.08	-.04	-.29	-.01	-.28

3.3. Correlational & linear regression analyses

We next examined the Pearson correlations between drift diffusion parameter estimates (as well as difference scores of split parameters), reaction time (and reaction time difference score), task performance (percent correct), frontal midline theta (FMT), and the residual FMT during the anti-saccade task. As shown in Table 2, drift rate during low- and high-conflict trials was significantly (positively) related mean FMT during low- and high-conflict conditions, respectively ($r = .76$, $P < .01$; $r = .69$, $P < .02$). Bias parameter estimates during low-conflict trials was significantly (negatively) associated with mean FMT during these trials

($r = -.75$, $P < .01$). Increased processing efficiency (i.e., drift rate) during high-conflict trials were related to increased FMT.

A single linear regression was conducted predicting mean FMT during the task to examine the assumption that drift diffusion parameter estimates provide additional information regarding cognitive control above-and-beyond simple reaction time. Thus, the first step included reaction time difference scores and the second step included both drift rate and bias difference scores. All predictor variables were centered prior to analysis. As shown in Table 3, the first step including only Δreaction time was not a significant predictor, $t(10) = 1.85$, $p = .10$. The second step significantly improved overall model fit, $\Delta F(3, 10) = 4.06$, $P < .05$,

Pro-Saccade Trials
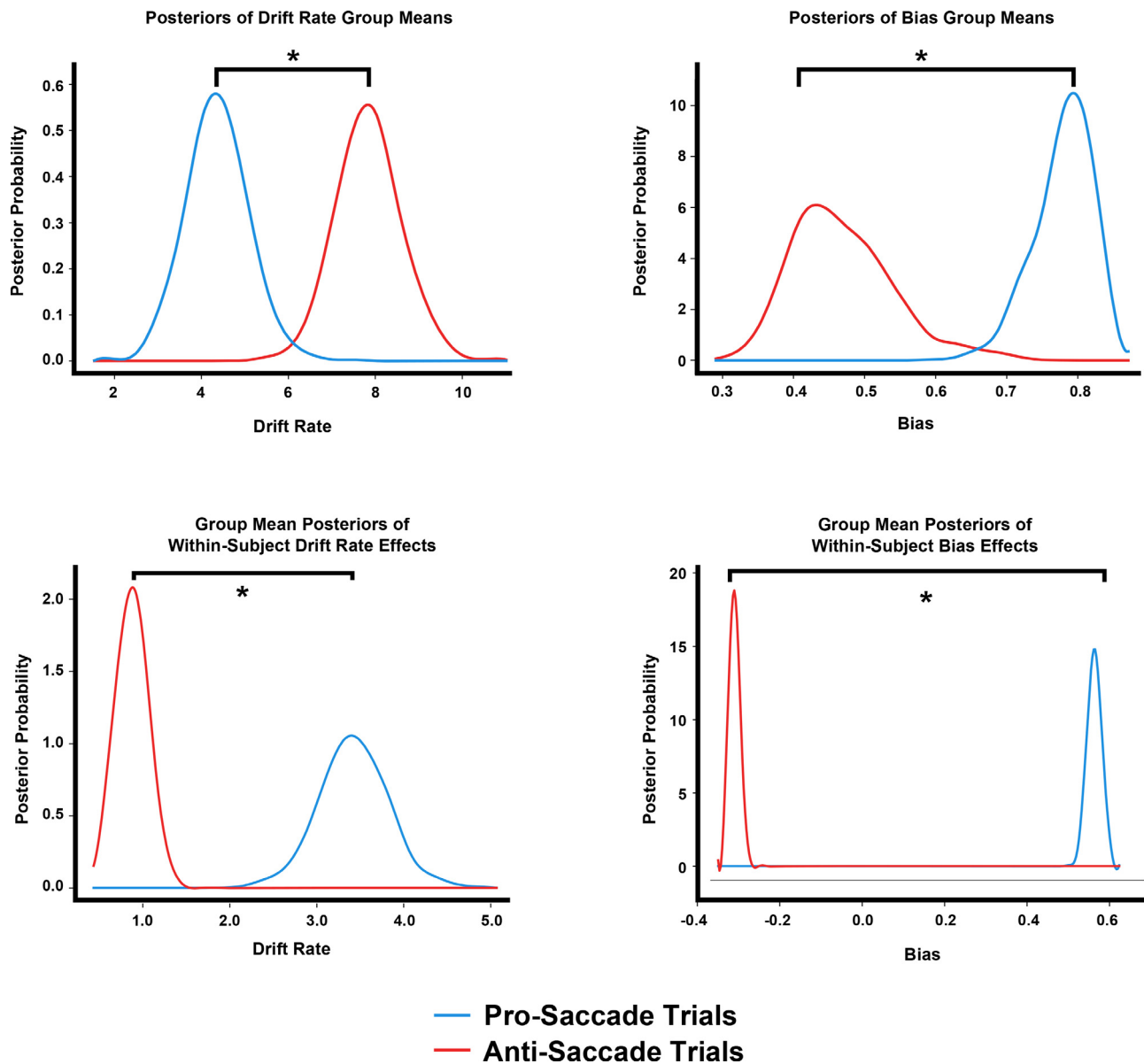**Anti-Saccade Trials**

Fig. 5. Posterior probabilities of drift rate (left) and bias (right) group means during pro-saccade (blue) and anti-saccade (red) trials (top); within-subject model group mean posterior probabilities of drift rate (left) and bias (right) during pro-saccade (blue) and anti-saccade (red) trials (bottom). The drift rate and bias posteriors depicted show the effect of the pro- and anti-saccade conditions on the parameter coefficients, where less distribution overlap indicates a larger conditional effect on the parameter estimate.

Table 3
Linear regression: reaction time (first step), bias, and drift rate(second step) predicting frontal midline theta during anti-saccade task. *Note.* Predictors were converted to z-scores; β = standardized beta; SE = standard error.

Frontal Midline Theta					95% CI	
	β	SE	t	p	Lower	Upper
1st Step						
ΔReaction Time	.32	.17	1.85	.10	-.07	.71
2nd Step						
ΔReaction Time	.17	.15	1.16	.29	-.18	.53
ΔBias	**.55**	**.21**	**2.63**	**.03**	**.05**	**1.04**
ΔDrift Rate	.40	.21	1.60	.09	-.09	.89
Model						
R^2	.64					
Adj. R^2	.48					
$F_{(3, 10)}$	4.06					

$\Delta R^2 = .64$, Adjusted $R^2 = .48$. While Δdrift rate was not a significant, predictor ($\beta = .40$, $t(10) = 1.60$, $p = .09$, $CI_{Lower} = -.09$, $CI_{Upper} = .89$), Δbias was a significant, positive predictor ($\beta = -.55$, $t(10) = 2.63$, $P < .05$, $CI_{Lower} = .05$, $CI_{Upper} = 1.04$) of FMT during the anti-saccade task.

3.4. Drift diffusion neural regressor model

Finally, we examined within-subject effects of trial-by-trial changes in FMT on drift rate and starting point bias parameters via a single drift diffusion regression model. The aforementioned pairs were informed by our previous correlation analyses and consistent with the best-fitting behavioral model, both drift rate and bias parameters were also allowed to function by condition within a single model. Instead of estimating a fixed parameter estimate per participant across trials, the regression model allows the respective parameter to vary on each trial as a function of their measured FMT activity during the task, as well as whether this effect interacts with the high-conflict condition (i.e., anti-saccade).
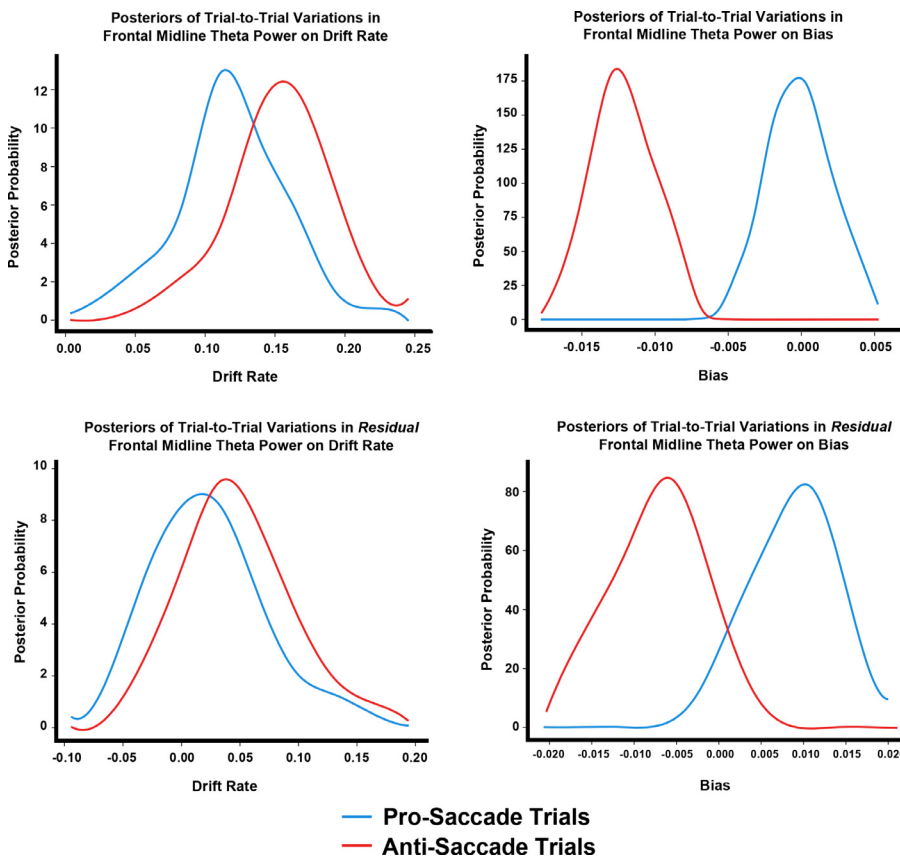
Fig. 6. Group mean posterior probabilities of frontal midline theta power within-subject effects on drift rate (left) and bias (right) during pro-saccade (blue) and anti-saccade (red) trials (top); group mean posterior probabilities of *residual* frontal midline theta power within-subject effects on drift rate (left) and bias (right) during pro-saccade (blue) and anti-saccade (red) trials (bottom). The drift rate posteriors show that the effect of trial-to-trial variations in frontal midline theta are to increase the estimated drift rate; the regression coefficient is positive for both conditions, and more than 99% of it is greater than zero (top left). The bias parameter posteriors (top right) show that the effect of trial-to-trial variations in frontal midline theta are to decrease the estimated bias but only for the anti-saccade condition; the regression coefficient of bias during the pro-saccade condition, in contrast, directly passes through zero.

Thus, the effect of FMT on parameter estimates is examined separately for low- and high-conflict trials. The posteriors depicted in Fig. 6 illustrate the effect of trial-to-trial variations in FMT on drift rate and bias parameter estimates, respectively. When the regression coefficient is positive (e.g., the posterior is meaningfully greater than zero) the effect of FMT is linked to increased parameter estimates; when negative, the effect of FMT is linked to decreases in parameter estimates. As shown in Fig. 6 (top), the drift rate in high-conflict trials increased in proportion to the degree of FMT ($P < .001$), as well as low-conflict trials ($P < .001$). However, the effect of FMT on drift rate did not meaningfully differ as a function of condition ($P = .42$). In contrast, bias during high conflict *decreased* in proportion to the level of FMT during high-conflict trials ($P < .001$), but this effect was absent during low conflict, as evidenced by the posterior distribution passing through zero. There was a meaningful difference between the effect of FMT on the starting point bias by task condition ($P < .001$). Importantly, a neural regression models replacing FMT with *residual* FMT were not meaningful; both posterior distributions passed through zero regardless of condition, indicating that there were no meaningful associations observed between residual FMT, drift rate, and bias during either the low- or high-conflict trials (see Fig. 6, bottom). In other words, trial-by-trial FMT sources captured meaningful variation in decision-making given that their removal gives rise to a loss of robust associations between the residual EEG source signal(s) and task behavior.

4. Discussion

To enhance our understanding of proactive cognitive control of gaze behavior, we combined a gaze-contingent cued anti-saccade eye-tracking paradigm with concurrent EEG assessment. We examined the relationship between trial-by-trial EEG theta dynamics and latent behavioral processes derived within a drift diffusion modeling framework. We hypothesized that individual differences in frontal midline theta (FMT) during the anti-saccade task would relate to changes in participants' response efficiency (drift rate), their starting point bias (bias parameter), and the amount of evidence needed for a decision (decision threshold) during the task. While theta rhythms are thought to be indicative of the need for a controlled behavioral response (Cavanagh and Shackman, 2015), we sought to build on our prior work indicating that this neural signature may also relate more strongly to being cued of an upcoming need to exercise cognitive control (van Noordt et al., 2017).

Our findings support the hypothesis that effortful control of gaze behavior relates to FMT through dissociated latent decision parameters of drift rate (processing efficiency) and the starting point bias during a cued anti-saccade task. We found support for our hypothesis at both between-condition (group) and within-subject (individual) level analyses. These results were also complimented by our correlational and regression analyses. Overall, our findings indicate that it is possible to predict variance in FMT, at a task- and trial-level through distinct latent decision processes. Specifically, latent parameters thought to capture processing efficiency and response bias (i.e., starting point bias parameter), were found to meaningfully relate to FMT during the gaze-contingent eye tracking paradigm (correlational analyses). However, our regression analyses indicate that variance associated with the starting point bias, and not drift rate nor reaction time, predicted participant's FMT response. Critically, we did not find any evidence of a relationship between FMT and traditional metrics of task performance such as mean reaction time. In other words, applying a drift diffusion model to gaze performance was necessary for the relationship between task behavior and FMT to become salient. Moreover, we did not find any link between model parameters and residual (non-medial frontal) EEG sources.

At a between-condition level, our finding is indicating trials requiring the inhibition of a prepotent gaze response (i.e., look *away* from the cue) increased efficiency in processing. It is possible that being cued of the upcoming difficult trial (i.e., anti-saccade, high conflict) prompted individuals to increase attentional resources to subsequent stimulus fea-

tures improving task proficiency. Cued (proactive) control also had a meaningful effect on participants starting point bias; during low conflict (i.e., pro-saccade trials), participants had a strong bias requiring little information to correctly provide a pro-saccade response. This bias was found to shift downward to a more neutral starting point during high conflict (i.e., anti-saccade trials), where approximately equal evidence was required for either response. Behaviorally, our model results may indicate that when cued of an upcoming challenge (i.e., proactive control), individuals attempt to compensate by processing the stimulus more efficiently, while also shifting their bias such that they are more neutral in responding (when compared to low-conflict trials); rather than needing little evidence to respond in one direction (and thus, much more to accumulate to respond alternatively), approximately equal amounts of information was needed for either decision (i.e., a middle starting point).

While not the conventional interpretation of the bias parameter as an implicit propensity to respond a certain way, its inclusion in the model is posited to facilitate in a stimulus-response mapping. An individual is presented with a cue indicating a low conflict response on relatively more trials, naturally leading to a bias towards needing less evidence to provide a pro-saccade response (and more information to anti-saccade). To overcome this tendency, after being cued of the upcoming high-conflict trial, our findings indicate that participants tended to shift their bias to a more neutral starting point; they need less evidence to respond correctly in an effort to overcome the strong bias fostered to provide a pro-saccade (low conflict) response. While individual differences in the decision threshold parameter reflects a cautious or hasty decision-making style – an identical magnitude of evidence is needed to choose either of the two options – the starting point bias favors one decision boundary to the detriment to the alternative boundary; less information is required to make a correct response, but more evidence is needed for an incorrect response (or contrariwise).

Additional evidence supporting our hypothesis that parameters reflecting underlying processes of controlled gaze behavior relate to task-based changes in FMT came from our regressor model of neural dynamics and task behavior at the individual level. The aim of these analyses was to examine whether within-subject changes in FMT throughout the task (i.e., trial-by-trial changes) were associated with variance fluctuations in response (gaze) preparation and effortful control of gaze behavior. We found that an individuals' trial-by-trial changes in drift rate under both trials varied as a function of FMT; more theta power was associated with an enhanced drift rate (i.e., increased processing efficiency). Interestingly, the effect of FMT on drift rate appears to be similar across both low- and high- conflict conditions.

Increased FMT was also related to goal-directed gaze behavior through the starting point bias, shifting participants' starting point to require less evidence to accumulate to make the anti-saccade response (and therefore, more information was needed to make an incorrect pro-saccade response). This is in contrast to low-conflict trials, where estimates of participants' starting point bias suggested a very strong preference for a (correct) pro-saccade response, and therefore, a great deal of evidence was needed to accumulate to incorrectly identify the trial as an anti-saccade. Consistent with our hypothesis regarding the utility of applying computational modeling to elucidate brain-behavior relationships, only the starting point bias parameter displayed incremental validity in predicting mean FMT, above-and-beyond that of both reaction time and drift rate. Taken together with our behavioral results, it may be speculated that while FMT is important in preparing an individual for a cued challenge, FMT likely does not solely account for the increase in subsequent processing efficiency. This would appear to be consistent with our regression results where drift rate did not predict FMT when accounting for variance related to the starting point bias and task reaction time.

Broadly, our results are consistent with that of Cavanagh and colleagues (Cavanagh et al., 2014) who utilized a hierarchical drift diffusion framework to model gaze behavior. They found independent con-

tributions of the drift rate and decision threshold parameters on task performance, although the starting point bias parameter was not explored. Task differences (i.e., probabilistic learning task) also make a direct comparison difficult. In another study, Tannous et al. (2019) also used a hierarchical drift diffusion framework to model a modified anti-saccade task, though these researchers did not conduct model comparison and focused strictly on differences in the drift rate parameter between groups. Thus, it is unknown if, similar to our findings, a model allowing both drift rate and starting point bias parameters to vary by condition was the best fit to participants' performance in their data.

These findings are comparable to those reported in stimulation studies of frontal midline theta, where increased activity has been shown to have positive impacts on behavior (i.e., behavioral adjustments following errors) (Klink et al., 2020, Voelker et al., 2021). Transcranial stimulation in the theta frequency range over frontal regions, specifically, have been found to cause immediate improvements in behavioral adjustments following errors (Reinhart et al., 2015). Notably, these positive effects on behavior were not solely accounted for by a change in speed versus accuracy tradeoff (Fusco et al., 2018), which is generally linked to the decision threshold parameter, and therefore, consistent with our findings implicating the importance of the starting point bias. These findings contribute to growing evidence of FMT as a robust marker of proactive cognitive control processes (Cavanagh and Shackman, 2015, Cavanagh and Frank, 2014, Eisma et al., 2021), consistent with a large literature linking FMT oscillations with responses during inhibitory control (Nigbur et al., 2012, Nigbur et al., 2011), resolution of competing responses (Oehrn et al., 2014) and adjusting response strategies to task demands (López et al., 2019, McKewen et al., 2020). Taken together, FMT may facilitate proactive cognitive control at the response preparation stage that either directly or indirectly affects one's response style through a bias in the amount of information needed to make a decision under conflict.

It is important to note how our results relate to recent models of adaptive cognitive control (Cohen, 2014, Verbeke and Verguts, 2021, Verguts, 2017). The sync model emphasizes the importance of three dimensions: intensity (i.e., the required strength of control), selectivity (i.e., the task-relevant and task-irrelevant stimuli considered), and time scale (i.e., proactive, or slow time scale, versus reactivity, or fast time scale) (Verbeke and Verguts, 2021). Briefly, the number of theta bursts from the medial frontal cortex determines the intensity of control required; the lateral frontal cortex, tracking the demands of a task, distributes theta bursts to eligible task-specific neural populations to facilitate gamma synchrony modulating the selectivity dimension of cognitive control (Verbeke and Verguts, 2021, Verbeke et al., 2021). Put simply, this model speculates that the medial and lateral frontal cortex determines the intensity and selectivity, respectively, of adaptive cognitive control. At the within-subject trial-by-trial level, we found that FMT power was positively associated with increased efficiency during both pro- and anti-saccade conditions, consistent with the medial frontal cortex generating more bursts of theta following a cue preparing the participant of an upcoming conflict (Senoussi et al., 2022). This may also relate to the shift in bias to a more neutral starting point, associated with increased FMT, and facilitating a less biased approach to responding when compared to pro-saccade trials. An alternative would be that the change in the starting point bias parameter may be indirectly related to FMT through the lateral frontal cortex, which is hypothesized to coordinate task rules and goals dictating behavior.

A number of study limitations should be noted. While we relied on a small sample of adults, we made efforts to mitigate potentially committing type one error such as adopting a more conservative critical p-value and utilizing robust estimation techniques for our neural analyses. Robust estimation has proven useful for dealing with small sample sizes and preventing issues that arise when violating assumptions of traditional parametric tests (Wilcox, 2011). Moreover, the utility of robust parameter estimates in EEG allow for greater control over measures of location, alpha levels, and unrepresentative confidence inter-

vals (Wilcox, 2011, Wilcox and Keselman, 2003), quantifying effects of event-related activity across all time points (Desjardins and Segalowitz, 2013, Rousselet et al., 2008). Nevertheless, readers should consider our findings with the understanding that some may reflect false positives. We also did not conduct a parameter recovery analysis, which is a significant limitation of the current study.

4.1. Implications and future directions

Our findings suggest that the addition of eye-tracking measures may be worth considering when investigating neural systems involved in processing efficiency (i.e., drift rate) (Gold and Shadlen, 2007, Hare et al., 2011, O'connell et al., 2012) and the starting point bias (Cavanagh et al., 2011, Domenech and Dreher, 2010, Fisher, 2021, Forstmann et al., 2010), not only during reinforcement-based decision paradigms (Cavanagh et al., 2011) but also, as we demonstrate here, tasks requiring proactive cognitive control. Such research on the neural dynamics and substrates that facilitate controlled and/or the inhibition of gaze has crucial implications for how gaze affects the value of choice alternatives (Smith and Krajbich, 2019, Mormann and Russo, 2021), purchasing decisions (Krajbich et al., 2012, Shimojo et al., 2003, Armel et al., 2008), moral judgments (Newell and Le Pelley, 2018), as well as attentional bias for threat in individuals suffering from anxiety disorders (Armstrong and Olatunji, 2012, Bar-Haim et al., 2007, Weierich et al., 2008) and/or major depression (Sears et al., 2011, Sears et al., 2010, Peckham et al., 2010). Further, given that some studies report the utility of including pupil dilation in conjunction with gaze (Cavanagh et al., 2014), along with their dissociable roles as correlates of attention function and performance, it would be beneficial to consider both gaze and pupil dilation in inhibitory control. Future studies directly comparing the neural correlates involved in cognitive control requiring different behavioral responses (i.e., a button press versus a saccade) would likely be beneficial to the larger literature.

Ethical approval

All procedures performed in studies involving human participants were in accordance with the ethical standards of the institutional and/or national research committee and with the 1964 Helsinki declaration and its later amendments or comparable ethical standards.

Informed consent

Informed consent was obtained from all individual participants included in the study.

Data Availability Statement

Raw participant task data, trial-by-trial frontal midline theta data, trial-by-trial residual frontal midline theta data, and hierarchical drift diffusion modeling (HDDM) scripts will be uploaded to a repository for anyone to access. HDDM scripts were directly accessed from: http://ski.clps.brown.edu/hddm_docs/ (Wiecki, Sofer, & Frank, 2013).

Declaration of Competing Interest

On behalf of all authors, the corresponding author states that there is no conflict of interest.

Credit authorship contribution statement

Peter J. Castagna: Conceptualization, Methodology, Software, Formal analysis, Writing – original draft, Writing – review & editing. **Stefon van Noordt:** Conceptualization, Formal analysis, Investigation, Resources, Data curation, Funding acquisition, Writing – review & editing. **Per B. Sederberg:** Conceptualization, Writing – review & editing,

Supervision. **Michael J. Crowley:** Conceptualization, Data curation, Writing – review & editing, Project administration, Funding acquisition, Supervision.

Data availability

Data will be made available on request.

References

Adams, R.A., Huys, Q.J., Roiser, J.P., 2016. Computational psychiatry: towards a mathematically informed understanding of mental illness. Journal of Neurology, Neurosurgery & Psychiatry 87 (1), 53–63.

Archambault, C., Tullo, D., Clark, E., Faubert, J., Bertone, A., 2021. Assessing the feasibility of a classroom-based visual attention training program targeting academics for students with extremely low IQ. Pilot and Feasibility Studies 7 (1), 1–14.

Armel, K.C., Beaumel, A., Rangel, A., 2008. Biasing simple choices by manipulating relative visual attention. Judgment and Decision Making 3 (5), 396–403.

Armstrong, T., Olatunji, B.O., 2012. Eye tracking of attention in the affective disorders: A meta-analytic review and synthesis. Clinical Psychology Review 32 (8), 704–723.

Aron, A.R., 2011. From reactive to proactive and selective control: developing a richer model for stopping inappropriate responses. Biological Psychiatry 69 (12), e55–e68.

Bar-Haim, Y., Lamy, D., Pergamin, L., Bakermans-Kranenburg, M.J., Van Ijzendoorn, M.H., 2007. Threat-related attentional bias in anxious and nonanxious individuals: a meta–analytic study. Psychological Bulletin 133 (1), 1.

Beard, C., Sawyer, A.T., Hofmann, S.G., 2012. Efficacy of attention bias modification using threat and appetitive stimuli: A meta-analytic review. Behavior Therapy 43 (4), 724–740.

Bell, M.D., Fiszdon, J.M., Bryson, G., 2009. Attention training in schizophrenia: differing responses to similar tasks. Journal of Psychiatric Research 43 (4), 490–496.

Boettcher, J., Leek, L., Matson, L., Holmes, E.A., Browning, M., MacLeod, C., Andersson, G., Carlbring, P., 2013. Internet-based attention bias modification for social anxiety: a randomised controlled comparison of training towards negative and training towards positive cues. PloS one 8 (9), e71760.

Braver, T.S., 2012. The variable nature of cognitive control: a dual mechanisms framework. Trends in Cognitive Sciences 16 (2), 106–113.

Bullmore, E.T., Suckling, J., Overmeyer, S., Rabe-Hesketh, S., Taylor, E., Brammer, M.J., 1999. Global, voxel, and cluster tests, by theory and permutation, for a difference between two groups of structural MR images of the brain. IEEE Transactions on Medical Imaging 18 (1), 32–42.

Cavanagh, J.F., Figueroa, C.M., Cohen, M.X., Frank, M.J., 2012. Frontal theta reflects uncertainty and unexpectedness during exploration and exploitation. Cerebral Cortex 22 (11), 2575–2586.

Cavanagh, J.F., Frank, M.J., 2014. Frontal theta as a mechanism for cognitive control. Trends in Cognitive Sciences 18 (8), 414–421.

Cavanagh, J.F., Frank, M.J., Klein, T.J., Allen, J.J., 2010. Frontal theta links prediction errors to behavioral adaptation in reinforcement learning. Neuroimage 49 (4), 3198–3209.

Cavanagh, J.F., Shackman, A.J., 2015. Frontal midline theta reflects anxiety and cognitive control: meta-analytic evidence. Journal of Physiology-Paris 109 (1-3), 3–15.

Cavanagh, J.F., Wiecki, T.V., Cohen, M.X., Figueroa, C.M., Samanta, J., Sherman, S.J., Frank, M.J., 2011. Subthalamic nucleus stimulation reverses mediofrontal influence over decision threshold. Nature Neuroscience 14 (11), 1462–1467.

Cavanagh, J.F., Wiecki, T.V., Kochar, A., Frank, M.J., 2014. Eye tracking and pupillometry are indicators of dissociable latent decision processes. Journal of Experimental Psychology: General 143 (4), 1476.

Cohen, M.X., 2014. A neural microcircuit for cognitive conflict detection and signaling. Trends in Neurosciences 37 (9), 480–490.

Cohen, M.X., Donner, T.H., 2013. Midfrontal conflict-related theta-band power reflects neural oscillations that predict behavior. Journal of Neurophysiology 110 (12), 2752–2763.

Collins, A.G., Shenhav, A., 2021. Advances in modeling learning and decision-making in neuroscience. Neuropsychopharmacology 1–15.

Cooper, P.S., Garrett, P.M., Rennie, J.L., Karayanidis, F., 2015. Task uncertainty can account for mixing and switch costs in task-switching. PloS one 10 (6), e0131556.

Cooper, P.S., Wong, A.S., McKewen, M., Michie, P.T., Karayanidis, F., 2017. Frontoparietal theta oscillations during proactive control are associated with goal-updating and reduced behavioral variability. Biological Psychology 129, 253–264.

De Loof, E., Vassena, E., Janssens, C., De Taeye, L., Meurs, A., Van Roost, D., Boon, P., Raedt, R., Verguts, T., 2019. Preparing for hard times: scalp and intracranial physiological signatures of proactive cognitive control. Psychophysiology 56 (10), e13417.

Debener, S., Thorne, J., Schneider, T., & Viola, F. (2010). Using ICA for the analysis of EEG data. In (Vol. 1). https://doi.org/10.1093/acprof:oso/9780195372731.003.0008

Desjardins, J.A., Segalowitz, S.J., 2013. Deconstructing the early visual electrocortical responses to face and house stimuli. Journal of Vision 13 (5), 22–22.

Desjardins, J.A., van Noordt, S., Huberty, S., Segalowitz, S.J., Elsabbagh, M., 2021. EEG Integrated Platform Lossless (EEG-IP-L) pre-processing pipeline for objective signal quality assessment incorporating data annotation and blind source separation. Journal of Neuroscience Methods 347, 108961.

Dickerson, S.S., Kemeny, M.E., 2004. Acute stressors and cortisol responses: a theoretical integration and synthesis of laboratory research. Psychological Bulletin 130 (3), 355.

Domenech, P., Dreher, J.-C., 2010. Decision threshold modulation in the human brain. Journal of Neuroscience 30 (43), 14305–14317.

Eisma, J., Rawls, E., Long, S., Mach, R., Lamm, C., 2021. Frontal midline theta differentiates separate cognitive control strategies while still generalizing the need for cognitive control. Scientific Reports 11 (1), 1–14.

Fiebelkorn, I.C., Kastner, S., 2019. A rhythmic theory of attention. Trends in Cognitive Sciences 23 (2), 87–101.

Finn, M., McDonald, S., 2011. Computerised cognitive training for older persons with mild cognitive impairment: a pilot study using a randomised controlled trial design. Brain Impairment 12 (3), 187–199.

Fisher, G., 2021. A multiattribute attentional drift diffusion model. Organizational behavior and Human Decision Processes 165, 167–182.

Fodor, L.A., Georgescu, R., Cuijpers, P., Szamoskozi, Ş., David, D., Furukawa, T.A., Cristea, I.A., 2020. Efficacy of cognitive bias modification interventions in anxiety and depressive disorders: a systematic review and network meta-analysis. The Lancet Psychiatry 7 (6), 506–514.

Forstmann, B.U., Brown, S., Dutilh, G., Neumann, J., Wagenmakers, E.-J., 2010. The neural substrate of prior information in perceptual decision making: a model-based analysis. Frontiers in Human Neuroscience 4, 40.

Fusco, G., Scandola, M., Feurra, M., Pavone, E.F., Rossi, S., Aglioti, S.M., 2018. Midfrontal theta transcranial alternating current stimulation modulates behavioural adjustment after error execution. European Journal of Neuroscience 48 (10), 3159–3170.

Gehring, W.J., Goss, B., Coles, M.G., Meyer, D.E., Donchin, E., 2018. The error-related negativity. Perspectives on Psychological Science 13 (2), 200–204.

Gelman, A., Rubin, D.B., 1992. Inference from iterative simulation using multiple sequences. Statistical Science 7 (4), 457–472.

Gentsch, A., Ullsperger, P., Ullsperger, M., 2009. Dissociable medial frontal negativities from a common monitoring system for self-and externally caused failure of goal achievement. Neuroimage 47 (4), 2023–2030.

Gold, J.I., Shadlen, M.N., 2007. The neural basis of decision making. Annual Review of Neuroscience 30, 535–574.

Groppe, D.M., Urbach, T.P., Kutas, M., 2011a. Mass univariate analysis of event-related brain potentials/fields I: A critical tutorial review. Psychophysiology 48 (12), 1711–1725.

Groppe, D.M., Urbach, T.P., Kutas, M., 2011b. Mass univariate analysis of event-related brain potentials/fields II: Simulation studies. Psychophysiology 48 (12), 1726–1737.

Habedank, I, Lennartz, S. J., Arslan, R. C., & Ertle, A. (2017). Online attention bias modification for Obsessive-Compulsive Disorder: A randomized controlled trial.

Hallion, L.S., Ruscio, A.M., 2011. A meta-analysis of the effect of cognitive bias modification on anxiety and depression. Psychological Bulletin 137 (6), 940.

Hare, T.A., Schultz, W., Camerer, C.F., O'Doherty, J.P., Rangel, A., 2011. Transformation of stimulus value signals into motor commands during simple choice. Proceedings of the National Academy of Sciences 108 (44), 18120–18125.

Herz, D.M., Zavala, B.A., Bogacz, R., Brown, P., 2016. Neural correlates of decision thresholds in the human subthalamic nucleus. Current Biology 26 (7), 916–920.

Hoffmann, S., Falkenstein, M., 2010. Independent component analysis of erroneous and correct responses suggests online response control. Human Brain Mapping 31 (9), 1305–1315.

Holroyd, C.B., Coles, M.G.H., 2002. The neural basis of human error processing: Reinforcement learning, dopamine, and the error-related negativity. Psychological Review 109 (4), 679–709. doi:10.1037/0033-295x.109.4.679.

Jaffard, M., Benraiss, A., Longcamp, M., Velay, J.-L., Boulinguez, P., 2007. Cueing method biases in visual detection studies. Brain Research 1179, 106–118.

Jaffard, M., Longcamp, M., Velay, J.-L., Anton, J.-L., Roth, M., Nazarian, B., Boulinguez, P., 2008. Proactive inhibitory control of movement assessed by event-related fMRI. Neuroimage 42 (3), 1196–1206.

Javadipour, S., Nejati, V., Yadegari, F., Javadipour, S., Fazele, S.A.A., 2018. A Visual Attention Training Program for the Improvement of Auditory Comprehension in Aphasia. NeuroQuantology 16 (4).

Jha, A., Diehl, B., Strange, B., Miserocchi, A., Chowdhury, F., McEvoy, A.W., Nachev, P., 2022. Orienting to fear under transient focal disruption of the human amygdala. Brain.

Joekar, S., Amiri, S., Birashk, B., Aghebati, A., 2017. Effectiveness of a visual attention training program on the reduction of ADHD symptoms in preschool children at risk for ADHD in Isfahan: a pilot study. Iranian Journal of Psychiatry and Behavioral Sciences 11 (4).

Kalfaoğlu, Ç., Stafford, T., Milne, E., 2018. Frontal theta band oscillations predict error correction and posterror slowing in typing. Journal of Experimental Psychology: Human Perception and Performance 44 (1), 69.

Klink, K., Paßmann, S., Kasten, F.H., Peter, J., 2020. The modulation of cognitive performance with transcranial alternating current stimulation: a systematic review of frequency-specific effects. Brain Sciences 10 (12), 932.

Kłosowska, J., Blaut, A., Paulewicz, B., 2015. The efficacy of determinants of attention bias training in mental disorders. Psychiatr. Pol 49 (6), 1169–1178.

Krajbich, I., Lu, D., Camerer, C., Rangel, A., 2012. The attentional drift-diffusion model extends to simple purchasing decisions. Frontiers in Psychology 3, 193.

López, M.E., Pusil, S., Pereda, E., Maestú, F., Barceló, F., 2019. Dynamic low frequency EEG phase synchronization patterns during proactive control of task switching. Neuroimage 186, 70–82.

Maris, E., 2004. Randomization tests for ERP topographies and whole spatiotemporal data matrices. Psychophysiology 41 (1), 142–151.

Maris, E., Oostenveld, R., 2007. Nonparametric statistical testing of EEG-and MEG-data. Journal of Neuroscience Methods 164 (1), 177–190.

Mas-Herrero, E., Marco-Pallarés, J., 2014. Frontal theta oscillatory activity is a common mechanism for the computation of unexpected outcomes and learning rate. Journal of Cognitive Neuroscience 26 (3), 447–458.

McKewen, M., Cooper, P.S., Wong, A.S., Michie, P.T., Sauseng, P., Karayanidis, F., 2020. Task-switching costs have distinct phase-locked and nonphase-locked EEG power effects. Psychophysiology 57 (5), e13533.

Mensen, A., Khatami, R., 2013. Advanced EEG analysis using threshold-free cluster-enhancement and non-parametric statistics. Neuroimage 67, 111–118.

Meyer, H.C., Bucci, D.J., 2016. Neural and behavioral mechanisms of proactive and reactive inhibition. Learning & Memory 23 (10), 504–514.

Mogg, K., Waters, A.M., Bradley, B.P., 2017. Attention bias modification (ABM): Review of effects of multisession ABM training on anxiety and threat-related attention in high--anxious individuals. Clinical Psychological Science 5 (4), 698–717.

Mormann, M., Russo, J.E., 2021. Does attention increase the value of choice alternatives? Trends in Cognitive Sciences.

Narayanan, N.S., Cavanagh, J.F., Frank, M.J., Laubach, M., 2013. Common medial frontal mechanisms of adaptive control in humans and rodents. Nature Neuroscience 16 (12), 1888–1895.

Nayak, S., Kuo, C., Tsai, A.C.-H., 2019. Mid-Frontal Theta Modulates Response Inhibition and Decision Making Processes in Emotional Contexts. Brain Sciences 9 (10), 271. https://www.mdpi.com/2076-3425/9/10/271.

Newell, B.R., Le Pelley, M.E., 2018. Perceptual but not complex moral judgments can be biased by exploiting the dynamics of eye-gaze. Journal of Experimental Psychology: General 147 (3), 409.

Nigbur, R., Cohen, M.X., Ridderinkhof, K.R., Stürmer, B., 2012. Theta dynamics reveal domain-specific control over stimulus and response conflict. Journal of Cognitive Neuroscience 24 (5), 1264–1274.

Nigbur, R., Ivanova, G., Stürmer, B., 2011. Theta power as a marker for cognitive interference. Clinical Neurophysiology 122 (11), 2185–2194.

O'Connell, R.G., Dockree, P.M., Kelly, S.P., 2012. A supramodal accumulation-to-bound signal that determines perceptual decisions in humans. Nature Neuroscience 15 (12), 1729–1735.

Oehrn, C.R., Hanslmayr, S., Fell, J., Deuker, L., Kremers, N.A., Lam, Do, A., T., Elger, C.E., Axmacher, N, 2014. Neural communication patterns underlying conflict detection, resolution, and adaptation. Journal of Neuroscience 34 (31), 10438–10452.

Oostenveld, R., Fries, P., Maris, E., Schoffelen, J.-M., 2011. FieldTrip: open source software for advanced analysis of MEG, EEG, and invasive electrophysiological data. Computational Intelligence and Neuroscience 2011.

Peckham, A.D., McHugh, R.K., Otto, M.W., 2010. A meta-analysis of the magnitude of biased attention in depression. Depression and Anxiety 27 (12), 1135–1142.

Ratcliff, R., 1978. A theory of memory retrieval. Psychological Review 85 (2), 59.

Ratcliff, R., 1985. Theoretical interpretations of the speed and accuracy of positive and negative responses. Psychological Review 92 (2), 212.

Ratcliff, R., Childers, R., 2015. Individual differences and fitting methods for the two–choice diffusion model of decision making. Decision 2 (4), 237.

Ratcliff, R., McKoon, G., 2008. The diffusion decision model: theory and data for two–choice decision tasks. Neural Computation 20 (4), 873–922.

Ratcliff, R., Rouder, J.N., 1998. Modeling response times for two-choice decisions. Psychological Science 9 (5), 347–356.

Ratcliff, R., Smith, P.L., Brown, S.D., McKoon, G., 2016. Diffusion decision model: Current issues and history. Trends in Cognitive Sciences 20 (4), 260–281.

Reinhart, R.M., 2017. Disruption and rescue of interareal theta phase coupling and adaptive behavior. Proceedings of the National Academy of Sciences 114 (43), 11542–11547.

Reinhart, R.M., Zhu, J., Park, S., Woodman, G.F., 2015. Synchronizing theta oscillations with direct-current stimulation strengthens adaptive control in the human brain. Proceedings of the National Academy of Sciences 112 (30), 9448–9453.

Roger, C., Bénar, C.G., Vidal, F., Hasbroucq, T., Burle, B., 2010. Rostral Cingulate Zone and correct response monitoring: ICA and source localization evidences for the unicity of correct-and error-negativities. Neuroimage 51 (1), 391–403.

Rousselet, G.A., Husk, J.S., Bennett, P.J., Sekuler, A.B., 2008. Time course and robustness of ERP object and face differences. Journal of Vision 8 (12), 3–3.

Sandre, A., Weinberg, A., 2019. Neither wrong nor right: Theta and delta power increase during performance monitoring under conditions of uncertainty. International Journal of Psychophysiology 146, 225–239.

Sauseng, P., Tschentscher, N., Biel, A.L., 2019. Be Prepared: Tune to FM-Theta for Cognitive Control. Trends in Neurosciences 42 (5), 307–309.

Sears, C.R., Newman, K.R., Ference, J.D., Thomas, C.L., 2011. Attention to emotional images in previously depressed individuals: An eye-tracking study. Cognitive Therapy and Research 35 (6), 517–528.

Sears, C.R., Thomas, C.L., LeHuquet, J.M., Johnson, J.C., 2010. Attentional biases in dysphoria: An eye-tracking study of the allocation and disengagement of attention. Cognition and Emotion 24 (8), 1349–1368.

Senoussi, M., Verbeke, P., Desender, K., De Loof, E., Talsma, D., Verguts, T., 2022. Theta oscillations shift towards optimal frequency for cognitive control. Nature Human Behaviour 1–14.

Shagan, S., Shagan, D., Shagan, B., Fiszdon, J.M., Thime, W., Haber, L.C., Pearlson, G.D., Choi, J., 2018. How music impacts visual attention training in schizophrenia: a pilot study. The Journal of Nervous and Mental Disease 206 (12), 968.

Shimojo, S., Simion, C., Shimojo, E., Scheier, C., 2003. Gaze bias both reflects and influences preference. Nature Neuroscience 6 (12), 1317–1322.

Smith, P.L., Ratcliff, R., 2004. Psychology and neurobiology of simple decisions. Trends in Neurosciences 27 (3), 161–168.

Smith, S.M., Krajbich, I., 2019. Gaze amplifies value in decision making. Psychological Science 30 (1), 116–128.

Spiegelhalter, D.J., Best, N.G., Carlin, B.P., Van Der Linde, A., 2002. Bayesian measures of model complexity and fit. Journal of the Royal Statistical Society: Series b (statistical methodology) 64 (4), 583–639.

Stone, M., 1960. Models for choice-reaction time. Psychometrika 25 (3), 251–260.

Tannous, J., Mwangi, B., Hasan, K.M., Narayana, P.A., Steinberg, J.L., Walss-Bass, C., Moeller, F.G., Schmitz, J.M., Lane, S.D., 2019. Measures of possible allostatic load in comorbid cocaine and alcohol use disorder: Brain white matter integrity, telomere length, and anti-saccade performance. PloS one 14 (1), e0199729.

Töllner, T., Wang, Y., Makeig, S., Müller, H.J., Jung, T.-P., Gramann, K., 2017. Two independent frontal midline theta oscillations during conflict detection and adaptation in a Simon-type manual reaching task. Journal of Neuroscience 37 (9), 2504–2515.

van Driel, J., Ort, E., Fahrenfort, J.J., Olivers, C.N.L., 2019. Beta and Theta Oscillations Differentially Support Free Versus Forced Control over Multiple-Target Search. Journal of Neuroscience 39 (9), 1733–1743. doi:10.1523/jneurosci.2547-18.2018.

van Noordt, S., Segalowitz, S.J., 2012. Performance monitoring and the medial prefrontal cortex: a review of individual differences and context effects as a window on self-regulation. Frontiers in Human Neuroscience 6, 197.

van Noordt, S.J., Desjardins, J.A., Segalowitz, S.J., 2015. Watch out! Medial frontal cortex is activated by cues signaling potential changes in response demands. Neuroimage 114, 356–370.

van Noordt, S.J.R., Desjardins, J.A., Gogo, C.E.T., Tekok-Kilic, A., Segalowitz, S.J., 2017. Cognitive control in the eye of the beholder: Electrocortical theta and alpha modulation during response preparation in a cued saccade task. Neuroimage 145, 82–95. doi:https://doi.org/10.1016/j.neuroimage.2016.09.054.

Verbeke, P., Ergo, K., De Loof, E., Verguts, T., 2021. Learning to synchronize: Midfrontal theta dynamics during rule switching. Journal of Neuroscience 41 (7), 1516–1528.

Verbeke, P., Verguts, T., 2021. Neural synchrony for adaptive control. Journal of Cognitive Neuroscience 33 (11), 2394–2412.

Verguts, T., 2017. Binding by random bursts: A computational model of cognitive control. Journal of Cognitive Neuroscience 29 (6), 1103–1118.

Voelker, P., Weible, A.P., Niell, C.M., Chavez, R.S., Tovar, D.T., Rothbart, M.K., Posner, M.I., 2021. Evaluating an Approach to Improving Attention Networks by Theta Stimulation. J*ournal of Physical Medicine and Rehabilitatio* 3 (1), 17.

Voss, A., Rothermund, K., Voss, J., 2004. Interpreting the parameters of the diffusion model: An empirical validation. Memory & Cognition 32 (7), 1206–1220. doi:10.3758/BF03196893.

Walsh, M.M., Anderson, J.R., 2012. Learning from experience: event-related potential correlates of reward processing, neural adaptation, and behavioral choice. Neuroscience & Biobehavioral Reviews 36 (8), 1870–1884.

Weierich, M.R., Treat, T.A., Hollingworth, A., 2008. Theories and measurement of visual attentional processing in anxiety. Cognition and Emotion 22 (6), 985–1018.

Wessel, J.R., Danielmeier, C., Morton, J.B., Ullsperger, M., 2012. Surprise and error: common neuronal architecture for the processing of errors and novelty. Journal of Neuroscience 32 (22), 7528–7537.

Wiecki, T.V., Antoniades, C.A., Stevenson, A., Kennard, C., Borowsky, B., Owen, G., Leavitt, B., Roos, R., Durr, A., Tabrizi, S.J., 2016. A computational cognitive biomarker for early-stage Huntington's disease. PloS one 11 (2), e0148409.

Wiecki, T.V., Sofer, I., Frank, M.J., 2013. HDDM: Hierarchical Bayesian estimation of the drift-diffusion model in Python. Frontiers in Neuroinformatics 7, 14.

Wilcox, R.R., 2011. Introduction to robust estimation and hypothesis testing. Academic press.

Wilcox, R.R., Keselman, H., 2003. Modern robust data analysis methods: measures of central tendency. Psychological Methods 8 (3), 254.

Winkler, I., Haufe, S., Porbadnigk, A.K., Müller, K.-R., Dähne, S., 2015. Identifying Granger causal relationships between neural power dynamics and variables of interest. Neuroimage 111, 489–504.

Womelsdorf, T., Johnston, K., Vinck, M., Everling, S., 2010. Theta-activity in anterior cingulate cortex predicts task rules and their adjustments following errors. Proceedings of the National Academy of Sciences 107 (11), 5248–5253.

Womelsdorf, T., Vinck, M., Leung, S.L., Everling, S., 2010. Selective theta-synchronization of choice-relevant information subserves goal-directed behavior. Frontiers in Human Neuroscience 4, 210.

Yeung, N., Botvinick, M.M., Cohen, J.D., 2004. The neural basis of error detection: conflict monitoring and the error-related negativity. Psychological Review 111 (4), 931.

Zuure, M.B., Hinkley, L.B., Tiesinga, P.H., Nagarajan, S.S., Cohen, M.X., 2020. Multiple midfrontal thetas revealed by source separation of simultaneous MEG and EEG. Journal of Neuroscience 40 (40), 7702–7713.